

Frequency dependence of the ac susceptibility in the random anisotropy system $\text{Dy}(\text{P}_{1-x}\text{V}_x)\text{O}_4$

A. J. Dirkmaat, D. Hüser,* G. J. Nieuwenhuys, and J. A. Mydosh

Kamerlingh Onnes Laboratorium, Rijks-Universiteit Leiden, 2300 RA Leiden, The Netherlands

P. Kettler† and M. Steiner

Hahn-Meitner-Institut, D-1000 Berlin 39, Federal Republic of Germany

(Received 24 October 1986)

From a detailed study of ac susceptibility measurements on the random anisotropy system $\text{Dy}(\text{P}_{1-x}\text{V}_x)\text{O}_4$, we have determined the magnetic phase diagram and characterized the various phases. In the intermediate-concentration range $0.26 \leq x \leq 0.83$, no long-range magnetic order has been found. Here our studies suggest a spin-glass-like phase. Additionally, we have studied the frequency dependence of the ac susceptibility (mainly the out-of-phase component χ'') over eight decades. From these measurements we have determined the distribution function of relaxation times as a function of temperature.

I. INTRODUCTION

In the past decade much work has been devoted to the study of magnetic transitions in random anisotropy systems, both theoretically and experimentally.¹⁻²⁷ Many of these studies have been devoted to site-random solid solutions in which two magnetic components with orthogonal spin anisotropies are present.¹⁻¹² For such systems a phase diagram showing a decoupled tetracritical point has been predicted theoretically,¹⁻² but this phase diagram has not been found experimentally.⁷⁻¹⁰ Much effort has also been given to systems with identical magnetic ions possessing site-dependent easy axes.¹³⁻²⁷ For materials in which the directions of the easy axes are randomly distributed so that the macroscopic magnetic behavior becomes isotropic, no long-range magnetic order is expected.¹⁴⁻¹⁶ Here a spin-glass state is predicted to occur, if the anisotropy is large enough.¹⁷⁻²¹ In addition, other magnetic ground states have been proposed.^{16,22,23} Experimental realizations of the systems investigated until now were mostly amorphous alloys comprising a rare-earth ion with an asymmetric charge distribution and a nonmagnetic host.²⁴⁻²⁶ In one of these systems a spin-glass state was observed.²⁶ Another representative of this kind of random anisotropy system is $\text{Dy}(\text{P}_{1-x}\text{V}_x)\text{O}_4$ which seems a favorable system in which to search for spin-glass properties in contrast to long-range magnetic order as a function of the ligand concentration x .

For all compositions $\text{Dy}(\text{P}_{1-x}\text{V}_x)\text{O}_4$ crystallizes in the tetragonal zircon structure with space group D_{4h}^{19} ($I4/amd$). A Jahn-Teller distortion occurs in DyVO_4 at 14 K, changing the tetragonal crystal structure into an orthorhombic one. In $\text{Dy}(\text{P}_{1-x}\text{V}_x)\text{O}_4$ the Dy^{3+} ions are surrounded by six VO_4^{3-} or PO_4^{3-} ions, which induce a crystalline electric field (CEF) at the sites of the Dy^{3+} ions. Because of the perturbation caused by this CEF on the electronic $4f$ states of the Dy^{3+} ions, the degeneracy with respect to J_z existing in free Dy^{3+} ions is removed and easy axes are created for the magnetic moments. In pure DyPO_4 the easy axis is directed along the c axis,

while in DyVO_4 it is along the a axis. In the mixed compounds the spin anisotropies are, in size and direction, randomly distributed over a large number of discrete possibilities.

The magnetic interactions between the Dy^{3+} ions are partly of exchange and partly of dipolar character. In particular, for DyVO_4 almost 88% of the interaction energy is known to be of dipolar nature,²⁸⁻³⁰ whereas in DyPO_4 it is only 33%.^{31,32} Because most theoretical studies on random anisotropy systems assume the interactions between the magnetic moments to be of the exchange type, one has to be careful with comparisons with theoretical predictions. In both pure compounds a transition to an antiferromagnetically-ordered state occurs in which the spins are aligned parallel to their respective easy axis.³³⁻³⁵ The transition temperatures for DyPO_4 and DyVO_4 are 3.4 K and 3.0 K, respectively. Previous experiments on the $\text{Dy}(\text{P}_{1-x}\text{V}_x)\text{O}_4$ system have shown that the admixture of the minority component decreases the preferred anisotropy.²⁷ For $x=0.40$ the bulk magnetization is isotropic. Elastic neutron scattering experiments²⁷ did not detect any long-range magnetic order perpendicular to the easy axis down to 0.45 K. For samples with concentrations $0.30 < x < 0.78$ no long-range magnetic order is found in either direction.

In the present paper we describe a systematic experimental study of the ac susceptibility of the $\text{Dy}(\text{P}_{1-x}\text{V}_x)\text{O}_4$ system. The ac susceptibility $\chi = \chi' - i\chi''$ has been measured as a function of frequency $\nu = \omega/2\pi$ ($3 \text{ Hz} \leq \nu \leq 6 \times 10^7 \text{ Hz}$), temperature T ($0.02 \text{ K} \leq T \leq 20 \text{ K}$) and concentration x ($0.08 \leq x \leq 0.97$). At certain concentrations and directions of the ac driving field our measurements show maxima at characteristic temperatures where no magnetic Bragg scattering, i.e., no long-range magnetic order has been observed in the neutron scattering experiments. In these cases the susceptibility behavior exhibits characteristic properties similar to those of spin glasses. Thus the temperatures at which the maxima in χ' occur are defined as the freezing temperatures T_f .

The main results of our investigation are as follows.

(i) The magnetic phase diagram shows a unique dependence of the freezing temperature on the ligand concentration and differs remarkably from those found for mixed systems in which two magnetic components with orthogonal spin anisotropies are present (Sec. III).

(ii) For $0.26 \leq x \leq 0.83$ and for all samples measured perpendicular to their respective easy axes we observe spin-glass-like properties. The susceptibility is frequency dependent for $T \lesssim T_f$. An analysis of the frequency dependences of χ'' measured at various temperatures shows that for $T < T_f$ the dependence is certainly not due to relaxation processes governed by a single relaxation time. For $x=0.40$ and $x=0.83$ the frequency dependences of $\chi''(T)$ are parametrized on the basis of a model,^{36,37} whose parameters determine a temperature-dependent distribution function of relaxation times. Hence a comparison with typical spin glasses can be made (Sec. IV).

II. EXPERIMENTAL TECHNIQUES

In order to cover wide ranges of temperatures and frequencies several experimental techniques have been utilized for the ac susceptibility. For measurements above 1.2 K three different arrangements were used for the particular frequency ranges. The low frequencies ($3 \text{ Hz} \leq \nu \leq 5 \times 10^3 \text{ Hz}$) were covered by a mutual inductance technique and the intermediate frequencies ($10^4 \text{ Hz} \leq \nu \leq 5 \times 10^5 \text{ Hz}$) by a self-inductance technique.³⁸ The in-phase and out-of-phase signals were simultaneously detected by means of a two-phase lock-in amplifier. In both setups we made use of a sample holder which consists of two separated compartments. One of them is filled with a paramagnetic salt [e.g., $\text{Mn}(\text{NH}_4)_2(\text{SO}_4)_2 \cdot 6\text{H}_2\text{O}$] and the other contains the sample to be investigated. This arrangement has the advantage that both setups could be calibrated at any temperature and frequency. At the highest frequencies ($3 \times 10^6 \text{ Hz} \leq \nu \leq 6 \times 10^7 \text{ Hz}$) the susceptibility was determined from the change of the impedance of a single coil when the sample is inserted. The signals were detected by means of a twin-T bridge, details of which are given in Ref. 39.

Temperatures in the range $0.02 \text{ K} \leq T \leq 4.2 \text{ K}$ were obtained by means of a dilution refrigerator.³⁶ Coil system, sample, and thermometer were situated inside the mixing chamber, so as to ensure good thermal contact. The mixing chamber was constructed out of epoxy resin to avoid eddy currents. In this temperature range the susceptibility was measured by a mutual inductance technique in the frequency range $2 \text{ Hz} \leq \nu \leq 2 \times 10^3 \text{ Hz}$ using a two-phase lock-in amplifier. The measurements were performed with an oscillating driving field h of $\approx 0.1 \text{ Oe}$. The calibration into absolute susceptibility units was performed by matching the data between 1.2 K and 4.2 K to those obtained at high temperatures.

The samples were flux grown at the Clarendon Laboratories, Oxford by Wankly⁴⁰ and were the same as those used in the neutron scattering experiments.²⁷ For our measurements we formed samples consisting of several needle-shaped crystals of approximate dimensions $1 \times 1 \times 4 \text{ mm}^3$ with a total mass of 25 mg.

III. THE MAGNETIC PHASE DIAGRAM

The temperature dependence of χ' measured along the c axis (χ'_{\parallel}) for the various samples is presented in Fig. 1(a) and perpendicular to the c axis (χ'_{\perp}) in Fig. 1(b). These measurements were performed in zero dc magnetic field at a frequency of 348 Hz. In agreement with the neutron scattering experiments, the samples with $x=0.08$ and $x=0.97$ show the characteristic antiferromagnetic temperature dependence of $\chi'(T)$ in their respective easy directions with a distinct inflection point, indicating the Néel temperature T_N , just below the susceptibility maximum. Perpendicular to the easy axis the susceptibility $\chi'(T)$ of these samples is very small ($x=0.08$) or even not detectable ($x=0.97$). However, for $x=0.08$ and $x=0.88$ a weak maximum in $\chi'(T)$ measured perpendicular to the easy axis is observed at a temperature much below T_N .

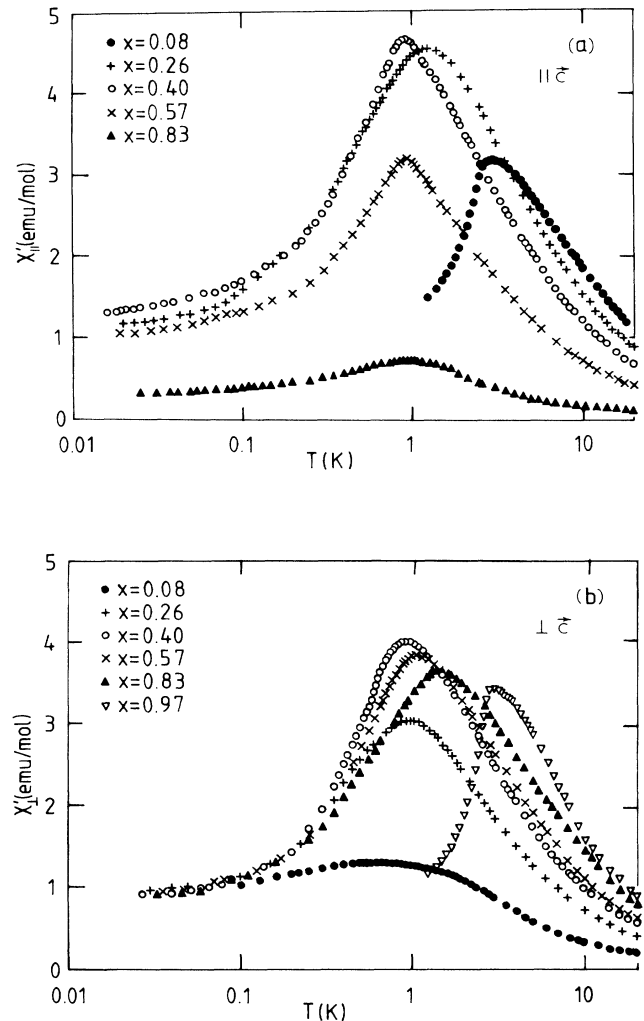


FIG. 1. The temperature dependence of $\chi'(T)$ for different concentrations x of $\text{Dy}(\text{P}_{1-x}\text{V}_x)\text{O}_4$ measured (a) parallel and (b) perpendicular to the c axis. The measurements have been performed in zero-magnetic field at a frequency of 348 Hz. Note the logarithmic temperature axis.

For an ideal Ising antiferromagnet the susceptibility perpendicular to the easy axis is zero. However, the admixture of the minority-ligand component creates randomly varying environments for the Dy^{3+} ions. Thereby, the pure Ising character is lost and below the Néel temperature a second kind of magnetic transition appears in $\chi'(T)$ perpendicular to the easy axis. At $T=20$ K (right-hand axes of Fig. 1) the susceptibility is found to be proportional to $1-x$ or x . Furthermore, the maximum value of χ' increases when the concentration x is changed from the pure substances $x=0$ or 1 towards $x=0.40$ at which concentration the material is magnetically isotropic. The shapes of the χ' curves become more symmetrical, i.e., less skewed, as $x=0.40$ is approached.

The transition temperatures T_N and T_f determined from susceptibility data, as well as the transition temperatures determined by neutron scattering, are collected in the phase diagram shown in Fig. 2. It displays some remarkable features. At both extremes of x a very strong decrease of the Néel temperature is found indicating that the long-range antiferromagnetic order is strongly affected by the admixture of the minority component. This behavior is in general agreement with the previously performed neutron scattering experiments.²⁷ At intermediate concentrations ($0.3 < x < 0.78$), and for all concentrations when measured perpendicular to the easy axis, no magnetic Bragg scattering has been observed in the neutron experiments down to $T=0.45$ K indicating the absence of long-range magnetic order.²⁷ However, the in-phase component $\chi'(T)$ exhibits well-defined maxima above 0.45 K, which we relate to a freezing process of randomly orient-

ed moments. Thus the system falls into the spinglass category. In the intermediate concentration range the x dependence of the freezing temperature T_f is extremely weak and the differences in the freezing temperatures determined parallel and perpendicular to the c axis are small. For $x=0.40$ no difference in T_f could be observed within our experimental accuracy of about 2%. As both ends of the phase diagram are approached T_f appears to bend towards zero.

IV. FREQUENCY DEPENDENCE OF THE SUSCEPTIBILITY

Similar to spin glasses the ac susceptibility of $\text{Dy}(\text{P}_{1-x}\text{V}_x)\text{O}_4$ for concentrations $0.26 \leq x \leq 0.83$ is frequency dependent. For the other concentrations, a frequency dependence of the susceptibility is observed, but only when measured perpendicular to the respective easy axis. As a typical example, the temperature dependence of $\chi'(T)$ and $\chi''(T)$ at several frequencies for a $\text{Dy}(\text{P}_{0.60}\text{V}_{0.40})\text{O}_4$ sample is shown in Fig. 3. At temperatures $T > 2$ K there are no differences in the in-phase components $\chi'(T)$ for the various measuring frequencies within the experimental accuracy. This feature plus the vanishing out-of-phase component $\chi''(T)$ and the increase of χ' with decreasing T indicate that the measured susceptibility χ' is the isothermal susceptibility $\chi(0)$. Decreasing the temperature, one observes a nonzero $\chi''(T)$ signal starting at the highest frequencies. Simultaneously, deviations in the $\chi'(T)$ signal from the isothermal value are evidenced. With decreasing frequency the freezing temperature shifts towards lower values.

For the samples with $x=0.83$ and $x=0.40$, the ac susceptibility perpendicular to the c axis has been measured over the full range of frequencies: $2 \text{ Hz} < \nu < 56 \times 10^6 \text{ Hz}$. The results for $\chi''_1(\omega)$, $\omega=2\pi\nu$, are presented in Fig. 4. For temperatures much higher than the freezing tempera-

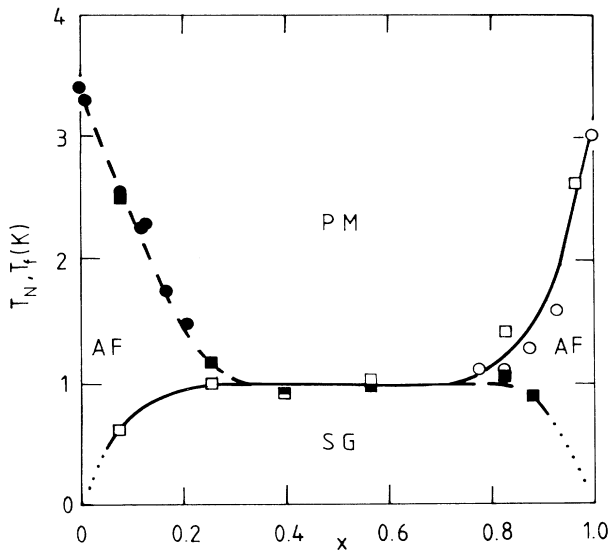


FIG. 2. The magnetic phase diagram of $\text{Dy}(\text{P}_{1-x}\text{V}_x)\text{O}_4$. The Néel temperatures T_N and freezing temperatures T_f have been determined by neutron scattering (\bullet, \circ) and susceptibility measurements (\blacksquare, \square). Solid symbols give T_N and T_f parallel to the c axis and open symbols perpendicular to the c axis. Coexistence occurs for $x \leq 0.3$ and $x \geq 0.8$.

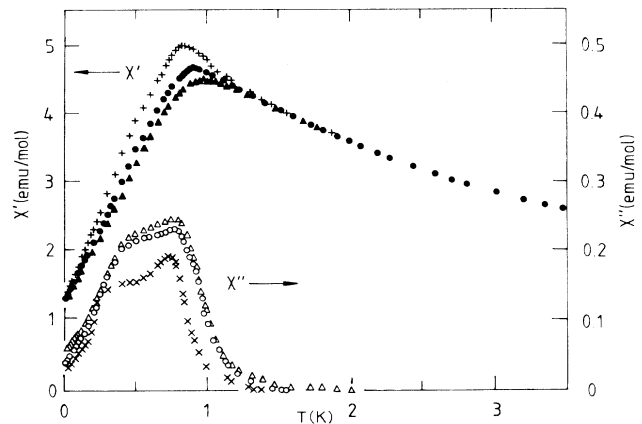


FIG. 3. Temperature dependence of $\chi'(T)$ ($+$, \bullet , and \blacktriangle) and $\chi''(T)$ (\times , \circ , and \triangle) for $\text{Dy}(\text{P}_{0.06}\text{V}_{0.40})\text{O}_4$ measured in zero-magnetic field for frequencies of 10.9 Hz ($+$, \times); 348 Hz (\bullet , \circ); 1969 Hz (\blacktriangle , \triangle). This sample has a fully isotropic susceptibility.

ture T_f , $\chi''(\omega)$ follows the Debye relation, so the frequency-dependent ac susceptibility can be written as

$$\chi(\omega) = \chi(\infty) + \frac{\chi(0) - \chi(\infty)}{1 + i\omega\tau}. \quad (1)$$

Here τ is the relaxation time and $\chi(0)$ is the isothermal susceptibility in the limit $\omega\tau \ll 1$. The susceptibility in the limit $\omega\tau \gg 1, \chi(\infty)$, is expected to be very small and is chosen to be zero in our further analysis. Since the measurements were performed in zero magnetic field the origin of the observed relaxation times must be a spin-spin relaxation process. Spin-spin relaxation was expected to be observed because in the pure systems, even in a magnetic field, spin-spin relaxation was established^{41,42} to be more important than spin-lattice relaxation for $T < 2.5$ K. This occurs in spite of the Ising character of the pure systems which is known to reduce the probability of spin-spin relaxation processes.

When one decreases the temperature through T_f , the low-frequency tail of the $\chi''(\nu)$ curves shifts up (see Fig. 4). At very low temperatures $\chi''(\nu)$ flattens out and has significant amplitude at low frequencies. Unfortunately, we were not able to measure above 2 kHz below 1 K, but the general frequency dependence seems to smoothly extrapolate to the maximum at approximately $\log \nu = 7.5$. This is illustrated by the broken lines in Fig. 4.

Since the frequency dependence of $\chi''(\nu)$ is considerably broader than that of a single Debye curve, the relaxation process cannot be described by a single relaxation time

constant. As is usually done in such situations a distribution function of relaxation time constants $g(\ln\tau)$ is introduced so that the frequency-dependent susceptibility can be written as

$$\frac{\chi(\omega)}{\chi(0)} = \int_{-\infty}^{\infty} \frac{g(\ln\tau)}{1 + i\omega\tau} d(\ln\tau). \quad (2)$$

From our experimental results it can be seen that $g(\ln\tau)$ approaches a δ -like function at temperatures above 4 K, where $\chi''(\nu)$ follows approximately a Debye curve. At low temperature $\chi''(\nu)$ clearly deviates from the Debye behavior, which means that $g(\ln\tau)$ becomes very broad, extending over many decades of time.

In order to compare our results with those obtained on other spin glasses we use a recently proposed phenomenological model^{36,37} for the frequency and temperature dependence of the susceptibility. In this model the distribution function for relaxation time constants is separated into two contributions. One is related to the "nearly free" spins exhibiting a relaxation time τ_f which is assumed to be temperature independent. This part can be described by a δ function $N_f \delta(\ln(\tau/\tau_f))$, where N_f is the fraction of "nearly free" spins. Thus the contribution of these spins to the susceptibility is given by a single Debye equation [Eq. (1)] with $\chi(\infty) = 0$, $\chi(0) = N_f \chi_f(0)$ and $\tau = \tau_f$ where $\chi_f(0)$ is the isothermal susceptibility of this part of the spin system.

A second contribution, related to the spins grouped into clusters, is described by a broad distribution of relaxation time constants $N_c g_c(\ln\tau)$ as in Eq. (2) where N_c is the fraction of clustered spins. Note that the term "cluster" is still applicable to the $\text{Dy}(\text{P}_{1-x}\text{V}_x)\text{O}_4$ system, but not in the sense of a spatial grouping of magnetic spins. Now there will be regions where, due to statistics, a nonvanishing average of the directions of the easy axes exists which enhances the correlation of the spins locally.

This distribution function $g_c(\ln\tau)$ results in a contribution to the susceptibility of the form

$$\Delta\chi(\omega) = \frac{N_c \chi_c(0)}{1 + (i\omega\tau_c)^{1-\alpha}}, \quad (3)$$

where $\chi_c(0)$ is the isothermal susceptibility of the clustered spin system and τ_c the average relaxation time constant. The quantity α determines the deviation from the Debye behavior. Using Eqs. (2) and (3), the distribution function $g_c(\ln\tau)$ can be derived viz.,

$$g_c(\ln\tau) = \frac{1}{2\pi} \frac{\sin(\alpha\pi)}{\cosh[(1-\alpha)\ln(\tau/\tau_c)] - \cos(\alpha\pi)}. \quad (4)$$

Note that α determines the width of the distribution function $g_c(\ln\tau)$. When $\alpha = 0$, this contribution to the susceptibility is described by a simple Debye equation. Since in the limit $\alpha \rightarrow 0$, $g_c(\ln\tau)$ becomes $\delta(\ln\tau/\tau_c)$. In the following we let $A = N_f \chi_f(0)$ and $B = N_c \chi_c(0)$. Then, from the sum of the two contributions to the susceptibility, the imaginary part can be extracted viz.,

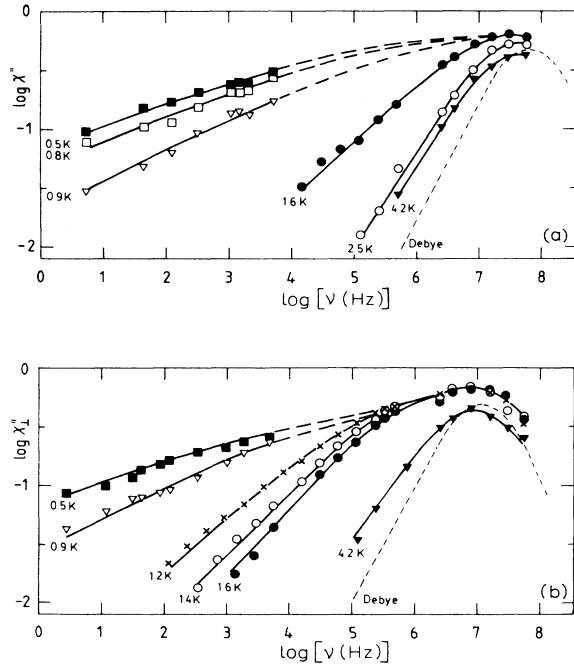


FIG. 4. $\chi''(\nu)$ as a function of frequency at several temperatures for $\text{Dy}(\text{P}_{1-x}\text{V}_x)\text{O}_4$: (a) $x = 0.40$; (b) $x = 0.83$ ($h \perp c$). The thin broken lines represent a Debye curve. The solid lines are fits to the data (see text for details).

$$\chi''(\omega) = \frac{A\omega\tau_f}{1 + \omega^2\tau_f^2} + \frac{B}{2} \frac{\cos(\frac{1}{2}\alpha\pi)}{\cosh((1-\alpha)\ln(\omega\tau_c)) + \sin(\frac{1}{2}\alpha\pi)} \quad (5)$$

The solid lines in Fig. 4 represent the fits of Eq. (5) to the data with the assumption that the relaxation time constant τ_f for the “free spins” is temperature independent. Hence the fitting procedure contains four parameters (A, B, α, τ_c) whose temperature dependence can be used to characterize the samples. The four parameters are only weakly correlated and all are determined to within 10%. In Fig. 5 the average relaxation time τ_c of the correlated spins is plotted as a function of the inverse temperature. As can be seen, τ_c obeys an Arrhenius law: $\tau_c = \tau_0 \exp(\Delta E/kT)$. For $1/T \rightarrow 0$ the solid lines extrapolate to $\tau_0 = 2.5 \times 10^{-9}$ s for $x=0.40$ and to $\tau_0 = 1.0 \times 10^{-8}$ s for $x=0.83$. The energy values, corresponding to the slopes in Fig. 6 are 0.9 K and 3.2 K, respectively. For the isotropic sample $\text{Dy}(\text{O}_{0.60}\text{V}_{0.40})\text{O}_4$ this energy is comparable with the freezing temperature $T_f = 0.85$ K. In the case of $\text{Dy}(\text{P}_{0.17}\text{V}_{0.83})\text{O}_4$ the energy value is close to the Néel temperature of the pure substance.

The temperature dependence of the parameters A (single spins) and B (correlated spins) are presented in Fig. 6. If the number of free spins (N_f) and the cluster sizes do not depend on temperature, one would expect that both contributions should be proportional to $1/T$. For $x=0.83$ we find $A \sim T^{-0.84}$ and $B \sim T^{-0.81}$, and for $x=0.40$ we have $A \sim T^{0.8}$ and $B \sim T^{-1.2}$. This means that the number of free spins and the number of correlated spins vary with temperature, similar to what has previously been observed in various spin glasses.³⁷ With decreasing temperature the number of free spins and correlated spins decreases for $x=0.83$, whereas for $x=0.40$ the number of correlated spins grows while the number of free spins decreases.

This difference can be explained as follows. For the sample with $x=0.83$ there is still a strong preference for

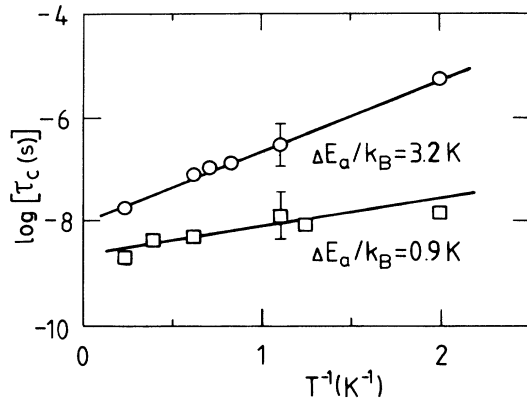


FIG. 5. Average relaxation time of the correlated spins τ_c as a function of the inverse temperature for $\text{Dy}(\text{P}_{1-x}\text{V}_x)\text{O}_4$: $x=0.40$ (\square); $x=0.83$ (\circ).

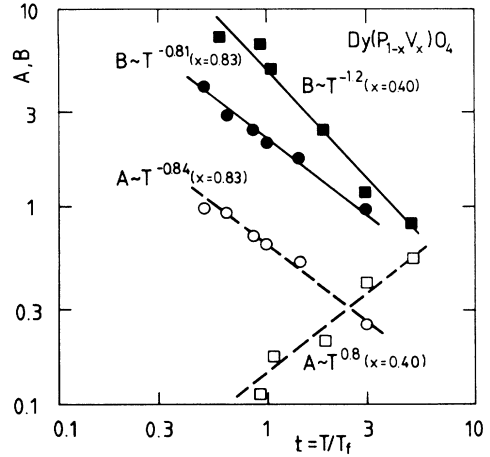


FIG. 6. Fit parameters A (open symbols) and B (solid symbols) as a function of the reduced temperature $t = T/T_f$ for two different concentrations of $\text{Dy}(\text{P}_{1-x}\text{V}_x)\text{O}_4$: $x=0.40$ (\blacksquare, \square), $x=0.83$ (\bullet, \circ).

the easy axis to be aligned perpendicular to the c axis, so that in large regions of the sample the spins can achieve a kind of imperfect antiferromagnetic order perpendicular to the c axis. Within the time scale of our measurement these giant clusters will appear to be inert, i.e., nonresponsive and therefore are not detected. However, with decreasing temperature the giant clusters will grow slightly and this accounts for the small decrease of the total number of spins contributing to the measurement. The formation of giant clusters also explains why the shorter time scale neutron scattering experiments detected a broadened antiferromagnetic transition, although results of the susceptibility at a much longer time scale clearly indicate some short-range magnetic order. In the isotropic sample with $x=0.40$, due to a random distribution of easy axes, there are only *finite* correlated regions. Consequently, the temperature dependences of A and B show a clear tenden-

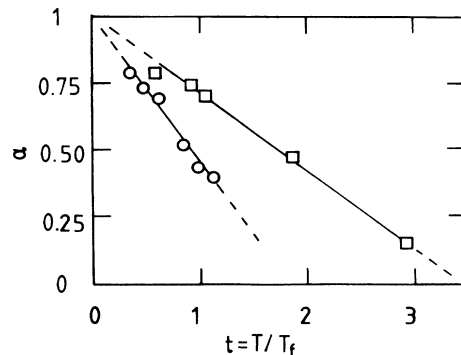


FIG. 7. Parameter α as a function of the reduced temperature $t = T/T_f$ for $\text{Dy}(\text{P}_{1-x}\text{V}_x)\text{O}_4$: $X=0.40$ (\square); $X=0.83$ (\circ).

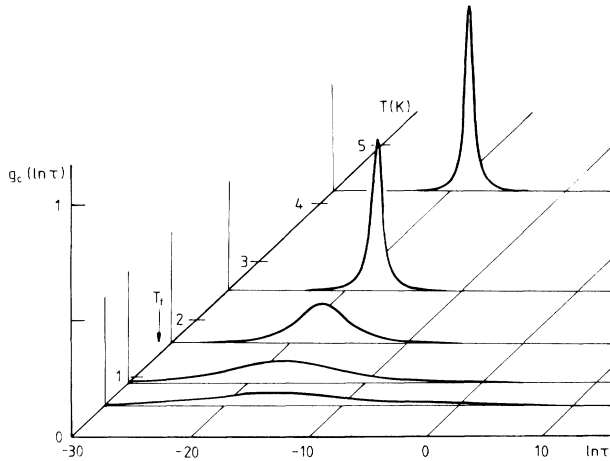


FIG. 8. The distribution function $g_c(\ln\tau)$ of relaxation time constants for $\text{Dy}(\text{P}_{0.60}\text{V}_{0.40})\text{O}_4$ at several temperatures.

cy for increasing the correlated regions at the expense of free spins as T is lowered below T_f .

The next step in our analysis is to calculate the distribution function $g_c(\ln\tau)$. First we focus our attention on the parameter α . In Fig. 7 this parameter is plotted as a function of the reduced temperature $t = T/T_f$. Both samples exhibit qualitatively the same behavior, namely a strongly T -dependent parameter α . Even above the freezing temperature T_f , a finite value for α is observed. This is attributed to the presence of short-range magnetically correlated regions which causes substantial deviations from paramagnetic behavior in spin glasses.⁴³ With decreasing temperature α increases linearly within our experimental accuracy, and extrapolated towards 1.0 as the reduced temperature approaches zero. Thus the distribution function becomes progressively broader with decreasing temperature, quite similar to the behavior observed in $\text{Cu}_{0.95}\text{Mn}_{0.05}$ and $(\text{Eu}_{0.4}\text{Sr}_{0.6})\text{S}$.³⁷

Finally, we have calculated the distribution function of relaxation time constants, which is presented in Fig. 8 for $\text{Dy}(\text{P}_{0.60}\text{V}_{0.40})\text{O}_4$. The results for the sample with $x = 0.83$ are quite similar. As is expected from the $\alpha(T)$ dependence in Fig. 7, there are relaxation time constants which clearly exceed those of noncorrelated or free spins even at temperatures $T \gg T_f$. If one passes T_f from above, the distribution function flattens, and long-time relaxation time constants become important which can easily exceed 1 s for the lowest temperatures.

V. DISCUSSION

On the basis of our ac-susceptibility measurements performed on the $\text{Dy}(\text{P}_{1-x}\text{V}_x)\text{O}_4$ system, it was possible to determine four phases: a paramagnetic phase, two antiferromagnetic phases, and a spin-glass phase. The Néel temperature of the pure materials is rapidly suppressed by a small admixture of the minority component. Already for $x = 0.26$ and $x = 0.83$ the transition to an antiferromagnetic order is smeared out and is accompanied by an on-

set of a $\chi''(T)$ component near T_N at low frequencies when measured along the easy axis, indicating the existence of short-range order. In a rather large range ($0.40 \leq x \leq 0.60$) the concentration dependences of the freezing temperatures are extremely weak. The freezing temperatures measured perpendicular to the respective easy axis seem to extrapolate to zero for $x = 0$ and $x = 1$. Thus the observed phase diagram shown in Fig. 2 is in marked contrast to the ones found for site-random solid solutions with two magnetic ions having orthogonal spin anisotropies, in which the weakest concentration dependence of the transition temperature is found at both ends of the diagram and the strongest is found near the tetracritical point.⁷⁻¹⁰

An interesting question arises from viewing the phase diagram in Fig. 2: for $x \leq 0.3$ or $x \geq 0.8$ in the low-temperature regime, is there a coexistence of antiferromagnetic long-range order with a transverse spin-glass freezing or a destruction of the antiferromagnetic order as the spin glass is formed, i.e., a "reentry" transition? In the neutron scattering experiments, for several ligand concentrations in the range mentioned above, samples were cooled to below the respective freezing temperature, determined from the ac-susceptibility results. Nevertheless none of the ligand concentrations showed a destruction of the antiferromagnetic order as the temperature was lowered to $T = 0.45$ K.²⁷ Thus we find that in the low-temperature phase for the $\text{Dy}(\text{P}_{1-x}\text{V}_x)\text{O}_4$ system, antiferromagnetic long-range order and a spin-glass behavior coexist. Such a coexistence has been observed previously for the Ising antiferromagnet-spin glass $\text{Fe}_{0.55}\text{Mg}_{0.45}\text{Cl}_2$.⁴⁴

The short-range order found for $x = 0.40$ and $x = 0.83$ (h.c.) may be described by employing a simple phenomenological model. For $x = 0.83$ the temperature dependences of the parameters A ($\sim T^{-0.81}$) and B ($\sim T^{-0.84}$) are qualitatively different from the dependences found for spin glasses like $\text{Eu}_{0.60}\text{Sr}_{0.40}\text{S}$ ($A \sim T, B \sim T^{-4}$) or $\text{Cu}_{0.95}\text{Mn}_{0.05}$ ($A \sim T^{0.5}, B \sim T^{-1.3}$).³⁷ With decreasing temperature the number of detected, correlated and non-correlated, spins is slightly reduced since a small amount of these spins align along the easy axis as a long-range-ordered, albeit imperfect, antiferromagnet. This also explains why the magnetic order was characterized by neutron scattering as antiferromagnetic long-range order without a sharp onset, whereas the ac-susceptibility measurements showed the existence of short-range order. The isotropic sample ($x = 0.40$) finally could be classified, in view of the results described in Ref. 37 for $\text{Cu}_{0.95}\text{Mn}_{0.05}$ and $\text{Eu}_{0.60}\text{Sr}_{0.40}\text{S}$, as a spin glass with a rather weak increase of the correlated regions when the temperature is decreased.

At this point it should be noted that both the $\text{Dy}(\text{P}_{1-x}\text{V}_x)\text{O}_4$ and the amorphous alloys already mentioned in the introduction only approximate the model system investigated in the theoretical work¹³⁻²³ where the interaction between the ions is taken to be a fully isotropic nearest-neighbor exchange and the only randomness introduced is the one in the directions of the easy axes. Thus the model Hamiltonian is

$$\mathcal{H} = -J \sum_{\langle i,j \rangle} \mathbf{S}_i \cdot \mathbf{S}_j - D \sum_i (\mathbf{S}_i \cdot \hat{\mathbf{n}}_i)^2. \quad (6)$$

J is the nearest-neighbor exchange-coupling constant, D is the anisotropy parameter, and \hat{n}_i is a unit vector aligned along the easy direction. The \hat{n}_i 's are distributed randomly over the unit sphere.

For the amorphous alloys^{24,26} the deviations from this model are twofold. The interactions between the magnetic ions are not simply due to nearest-neighbor exchange coupling but are presumably rather like an RKKY interaction. Furthermore, the randomness in the directions of the easy axes is accompanied by a randomness in structure and site occupancy. For the Dy(P_{1-x}V_x)O₄ the situation appears to be better because here the Dy ions are placed on a regular lattice. Now, however, there is a complex mixture of anisotropic exchange and dipolar interactions between the Dy³⁺ ions which also makes this system more complicated than the model system.

Regarding the two antiferromagnetically-ordered pure systems, as a first approximation the model Hamiltonian might be applied. If this is done then the exchange-coupling parameter should be taken negative instead of the positive one used in the theoretical work. This Hamiltonian can be transferred in the limit $D \rightarrow \infty$ in a random bond Ising Hamiltonian,

$$\mathcal{H} = \sum_{\langle i,j \rangle} -JS^2(\hat{n}_i \cdot \hat{n}_j)\sigma_i\sigma_j, \quad (7)$$

where $S_i = S\hat{n}_i\sigma_i$ with $\sigma_i = \pm 1$, $JS^2(\hat{n}_i \cdot \hat{n}_j)$ being the random exchange-coupling constant. As Jayaprakash and

Kirkpatrick¹⁶ noted the Hamiltonian (7) would lead to an energy

$$E = \frac{1}{2}JNS^2 - \frac{1}{2}JNS^2 \left| \sum_i \hat{n}_i\sigma_i \right|^2 \quad (8)$$

in the limit $D \rightarrow \infty$ and infinite range interactions. For systems with positive exchange-coupling parameters this would lead to a ground state having a maximum magnetization obtained by aligning the spins so that they all point in the same hemisphere.¹⁶ For systems with negative exchange-coupling parameters this would lead to a ground state having zero spontaneous magnetization. Thus the spin-glass state would be of the same energy as an approximate antiferromagnetically-ordered state. From this discussion, spin-glass behavior is expected for the Dy(P_{1-x}V_x)O₄ system, in particular since the nearest-neighbor exchange and dipolar interactions decrease strongly with distance.

ACKNOWLEDGMENTS

The authors would like to acknowledge J. C. Verstelle and A. J. van Duyneveldt for stimulating discussions and their interest in this work. We are also grateful to J. J. Baalbergen and J. van den Berg for their competent assistance with the measurements. This work was financially supported by the Nederlandse Stichting voor Fundamenteel Onderzoek der Materie (FOM).

*Present address: ERNO Raumfahrttechnik GmbH, BRD-2800 Bremen 1, Federal Republic of Germany.

†Present address: Sisto Didaktik GmbH, BRD-7300 Esslingen, Federal Republic of Germany.

¹A. Aharony and S. Fishman, Phys. Rev. Lett. **37**, 1587 (1976).

²S. Fishman and A. Aharony, Phys. Rev. B **18**, 3507 (1978).

³K. Katsumata, M. Kobayashi, and H. Yoshizawa, Phys. Rev. Lett. **43**, 960 (1979).

⁴A. Ito, Y. Someya, and K. Katsumata, Solid State Commun. **36**, 681 (1980).

⁵K. Katsumata, M. Yoshizawa, G. Shirane, and R. J. Birgeneau, Phys. Rev. B **31**, 316 (1985).

⁶L. Bevaart, E. Frikkee, J. V. Lebesque, and L. J. de Jongh, Phys. Rev. B **18**, 3376 (1978).

⁷A. Ito, S. Morimoto, Y. Someya, H. Ikeda, Y. Syono, and H. Takei, Solid State Commun. **41**, 507 (1982).

⁸A. Ito, S. Morimoto, Y. Someya, Y. Syono, H. Takei, J. Phys. Soc. Jpn. **51**, 3173 (1982).

⁹K. Katsumata, J. Tuchendler, and S. Legrand, Phys. Rev. B **30**, 1377 (1984).

¹⁰P. Wong, P. M. Horn, R. J. Birgeneau, and G. Shirane, Phys. Rev. B **27**, 428 (1983).

¹¹F. Matsubara and S. Inawashiro, J. Phys. Soc. Jpn. **42**, 1529 (1977).

¹²M. Oku and H. Igarashi, Prog. Theor. Phys. **70**, 1493 (1983).

¹³R. Harris, M. Plischke, and M. J. Zuchermann, Phys. Rev. Lett. **31**, 160 (1973).

¹⁴A. Aharony, Phys. Rev. B **12**, 1038 (1975).

¹⁵J. H. Chen and T. C. Lubensky, Phys. Rev. B **16**, 2106 (1977).

¹⁶C. Jayaprakash and S. Kirkpatrick, Phys. Rev. B **21**, 4072 (1980).

¹⁷R. A. Pelcovits, E. Pytte, and J. Rudnick, Phys. Rev. Lett. **40**, 476 (1978); **48**, 1297(E) (1982).

¹⁸R. A. Pelcovits, Phys. Rev. B **19**, 465 (1979).

¹⁹S. L. Ginzburg, Zh. Eksp. Teor. Fiz. **81**, 1389 (1981) [Sov. Phys.—JETP **54**, 737 (1981)].

²⁰Y. Y. Goldschmidt, Nucl. Phys. B **225**, 123 (1983).

²¹Y. Y. Goldschmidt, Phys. Rev. B **30**, 1632 (1984).

²²A. Aharony and E. Pytte, Phys. Rev. Lett. **45**, 1583 (1980).

²³B. Derrida and J. Vannimenus, J. Phys. C **13**, 3261 (1980).

²⁴J. M. B. Coey, J. Appl. Phys. **49**, 1646 (1978).

²⁵S. von Molnar, B. Barbara, T. R. McGuire, and R. Gambino, J. Appl. Phys. **53**, 2350 (1982).

²⁶T. Mizoguchi, T. R. McGuire, S. Kirkpatrick, and R. J. Gambino, Phys. Rev. Lett. **38**, 89 (1977).

²⁷P. Kettler, W. Steiner, H. Dachs, R. Germer, and B. Wanklyn, Phys. Rev. Lett. **47**, 1329 (1981).

²⁸A. H. Cooke, D. M. Martin, and M. R. Wells, Solid State Commun. **9**, 319 (1971).

²⁹G. A. Gehring, A. P. Malozemoff, W. Staude, and R. N. Tyte, J. Phys. Chem. Solids **33**, 1499 (1972).

³⁰A. Kasten and J. P. Becker, J. Phys. C **7**, 3120 (1974).

³¹C. J. Ellis, M. J. M. Leask, D. M. Martin, and M. R. Wells, J. Phys. C **4**, 2937 (1971).

³²G. A. Prinz, J. F. L. Lewis, and R. J. Wagner, Phys. Rev. B **10**, 2907 (1974).

³³W. Scharenberg and G. Will, Int. J. Magn. **1**, 277 (1971).

³⁴J. C. Wright, H. W. Moos, J. H. Colwell, B. W. Mangum, and D. D. Thornton, Phys. Rev. B **3**, 843 (1971).

³⁵G. Will and W. Schäfer, J. Phys. C **4**, 811 (1971).

³⁶D. Hüser, Ph. D. thesis, University of Leiden, 1985 (unpublished).

- ³⁷D. Hüser, A. J. van Duyneveldt, G. J. Nieuwenhuys, and J. A. Mydosh, *J. Phys. C* **19**, 3697 (1986).
- ³⁸A. J. van Duyneveldt, *J. Appl. Phys.* **53**, 8006 (1982).
- ³⁹R. C. Rutten, J. Verstelle, and N. J. Poulis, *Physica (Amsterdam)* **121B**, 351 (1983).
- ⁴⁰S. H. Smith and B. M. Wanklyn, *J. Cryst. Growth* **21**, 23 (1974).
- ⁴¹A. Kasten, P. H. Müller, and M. Schienle, *Physica* **114B**, 77 (1982).
- ⁴²M. Schienle, A. Kasten, and P. H. Müller, *Phys. Status Solidi B* **119**, 611 (1983).
- ⁴³A. F. J. Morgownik and J. A. Mydosh, *Solid State Commun.* **47**, 321 (1983).
- ⁴⁴Po-zen Wong, S. von Molnar, T. T. M. Palstra, J. A. Mydosh, H. Yoshizawa, S. M. Shapiro, and A. Ito, *Phys. Rev. Lett.* **55**, 2043 (1985).